Acta Crystallographica Section F
Structural Biology and Crystallization Communications
ISSN 1744-3091

Crystallization and preliminary X-ray crystallographic analysis of human quinolinate phosphoribosyltransferase

Gil Bu Kang,[a]‡ Mun-Kyoung Kim,[a]‡ Hyung-Seop Youn,[a] Jun Yop An,[a] Jung-Gyu Lee,[a] Kyoung Ryoung Park,[a] Sung Hang Lee,[b] Yongseong Kim,[c] Shin-Ichi Fukuoka[d] and Soo Hyun Eom[a]*

[a]School of Life Sciences, Gwangju Institute of Science and Technology, Gwangju 500-712, Republic of Korea, [b]Research Center for Resistant Cells, Chosun University Medical School, Gwangju, Republic of Korea, [c]Department of Chemistry, Kyungnam University, Wolyoun-dong, Masan 631-701, Republic of Korea, and [d]Laboratory of Molecular Cell Biology, Department of Chemistry and Biological Science, College of Science and Engineering, Aoyama Gakuin University, 5-10-1 Fuchinobe, Sagamihara, Kanagawa 229-8558, Japan

‡ These authors contributed equally to this work.

Correspondence e-mail: eom@gist.ac.kr

Received 20 January 2010
Accepted 12 October 2010

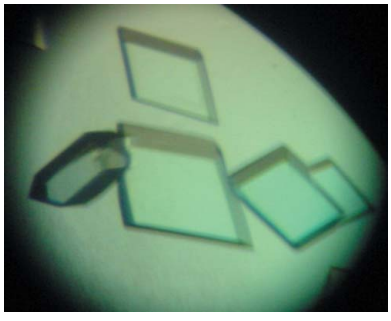

Quinolinate phosphoribosyltransferase (QPRTase) is a key NAD-biosynthetic enzyme which catalyzes the transfer of quinolinic acid to 5-phosphoribosyl-1-pyrophosphate, yielding nicotinic acid mononucleotide. *Homo sapiens* QPRTase (*Hs*-QPRTase) appeared as a hexamer during purification and the protein was crystallized. Diffraction data were collected and processed at 2.8 Å resolution. Native *Hs*-QPRTase crystals belonged to space group $P2_1$, with unit-cell parameters $a = 76.2$, $b = 137.1$, $c = 92.7$ Å, $\beta = 103.8^\circ$. Assuming the presence of six molecules in the asymmetric unit, the calculated Matthews coefficient is 2.46 Å^3 Da^{-1}, which corresponds to a solvent content of 49.9%.

1. Introduction

Quinolinate phosphoribosyltransferase (QPRTase) is an essential enzyme for the *de novo* biosynthesis of nicotinamide adenine dinucleotide (NAD) in both prokaryotes and eukaryotes (Foster & Moat, 1980). This enzyme catalyzes the formation of nicotinic acid mononucleotide (NAMN), pyrophosphate and CO_2 from quinolinic acid (QA) and 5-phosphoribosyl-1-pyrophosphate (PRPP) in a reaction that involves phosphoribosyl transfer followed by decarboxylation. QA is the first intermediate in this biosynthetic process. In eukaryotes QA is produced *via* degradation of tryptophan, while in prokaryotes it is produced from dihydroxylacetone phosphate and L-aspartate. Notably, QA is a known neurotoxin in mammals: its action is exerted *via* sustained activation of glutamate *N*-methyl-D-aspartate receptors and it is involved in a variety of neurological diseases (Foster *et al.*, 1985; Foster & Schwarcz, 1985; Feldblum *et al.*, 1988).

The structures of QPRTase from *Homo sapiens*, *Saccharomyces cerevisiae*, *Helicobacter pylori*, *Thermus thermophilus*, *Mycobacterium tuberculosis*, *Salmonella typhimurium* and *Thermotoga maritima* have all been shown to consist of an N-terminal four-stranded open-face β-sandwich domain and a C-terminal α/β-barrel domain (Eads *et al.*, 1997; Sharma *et al.*, 1998; Schwarzenbacher *et al.*, 2004; Kim *et al.*, 2006; Liu *et al.*, 2007; di Luccio & Wilson, 2008). QPRTases exist as dimers or hexamers; those from eukaryotes, including yeast, hog, rat and human, are hexamers in solution (Iwai & Taguchi, 1974; Okuno & Schwarcz, 1985; Okuno *et al.*, 1988; di Luccio & Wilson, 2008). Consistent with these findings, structural studies of QPRTases from *Homo sapiens* and *Saccharomyces cerevisiae* showed that they form a hexameric structure (Liu *et al.*, 2007; di Luccio & Wilson, 2008). In contrast, most QPRTases from prokaryotes, including those from *M. tuberculosis*, *Salmonella typhimurium* and *Thermotoga maritima*, are dimeric, although some prokaryotic QPRTases (those from *Helicobacter pylori* and *Thermus thermophilus*) have a hexameric structure identical to the enzymes from *Homo sapiens* and *Saccharomyces cerevisiae*.

The reaction catalyzed by QPRTase is central and indispensable to NAD biosynthesis and cell survival in prokaryotes. Thus, QPRTases from bacterial pathogens such as *Helicobacter pylori*, *M. tuberculosis* and *S. typhimurium* represent attractive targets for antibacterial drugs (Eads *et al.*, 1997; Sharma *et al.*, 1998; Kim *et al.*, 2006) and structural information about the host QPRTase is essential for the

proper design of specifically antibacterial inhibitors. Currently, only the structure of *Homo sapiens* QPRTase (*Hs*-QPRTase) in complex with a tartrate molecule, which partly mimics QA, is available (Liu *et al.*, 2007). Once we know the apo structure of *Hs*-QPRTase, we should be able to determine the mechanism underlying substrate recognition and provide structural information for drug development. As a first step towards this goal, we report here the overexpression, purification and crystallization of apo *Hs*-QPRTase and its preliminary X-ray characterization.

2. Materials and methods

2.1. Expression and purification

DNA encoding *Hs*-QPRTase (residues 1–297) was amplified by PCR and subcloned into the *Nde*I and *Xho*I sites of the expression vector pET-21a (Novagen). After transformation into *Escherichia coli* strain C41 (DE3), recombinant *Hs*-QPRTase was induced by treating the cells with 1 m*M* isopropyl β-D-1-thiogalactopyranoside (IPTG) for 6 h at 310 K. The cells were then harvested and resuspended in lysis buffer containing 50 m*M* sodium phosphate pH 7.5, 300 m*M* NaCl, after which the suspended cells were lysed by sonication and centrifuged at 14 000*g* for 1 h. The supernatant was collected and loaded onto a column packed with Ni–NTA resin (Peptron) pre-equilibrated with lysis buffer. After washing with wash buffer (50 m*M* sodium phosphate pH 7.5, 300 m*M* NaCl, 10 m*M* imidazole), the bound protein was eluted with elution buffer (50 m*M* sodium phosphate pH 7.5, 300 m*M* NaCl, 250 m*M* imidazole). The *Hs*-QPRTase protein was then further purified by size-exclusion chromatography on a Superdex 200 column (Pharmacia) equilibrated with 20 m*M* HEPES–NaOH pH 7.5, 100 m*M* KCl. The fractions containing the recombinant protein were pooled and concentrated to 15 mg ml^{-1} using a Centriprep-10 (Amicon).

2.2. Crystallization and data collection

Full-length *Hs*-QPRTase (residues 1–297), supplemented with an additional Leu and Glu and a hexahistidine tag at its C-terminus, was crystallized at room temperature (294 $\pm$ 1 K) using the hanging-drop vapour-diffusion method. The crystals were grown on a siliconized cover slip by equilibrating a mixture consisting of 1 µl protein solution (15 mg ml^{-1} protein in 20 m*M* HEPES–NaOH pH 7.5, 100 m*M* KCl) and 1 µl reservoir solution [100 m*M* MES–NaOH pH 5.0, 7–15%(*w*/*v*) PEG MME 2K, 10 m*M* KSCN] against 500 µl reservoir solution. Plate-like single crystals grew to maximum dimensions of 0.3 $\times$ 0.3 $\times$ 0.1 mm over the period of a week (Fig. 1). They were cryoprotected in reservoir solution supplemented with 25%(*v*/*v*) glycerol and flash-cooled under N_2 gas at 95 K. Native data were collected to 2.8 Å resolution from a single frozen crystal using an ADSC Quantum 210 CCD detector on beamline NW12 of Photon Factory (Tsukuba, Japan). The data set was processed and scaled using *HKL*-2000 (Otwinowski & Minor, 1997). The data-collection statistics are summarized in Table 1.

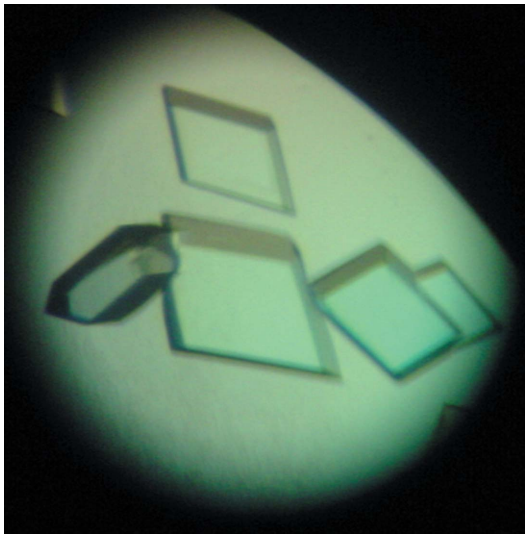

Figure 1
Native crystals of *Hs*-QPRTase grown for 7 d in 100 m*M* MES–NaOH pH 5.0, 7–12%(*w*/*v*) PEG MME 2K, 10 m*M* KSCN. The crystal dimensions are approximately 0.3 $\times$ 0.3 $\times$ 0.1 mm.

Table 1
Data-collection statistics.

Values in parentheses are for the highest resolution shell.

X-ray source	PF-AR NW12
Wavelength (Å)	1.0000
Space group	$P2_1$
Unit-cell parameters (Å, °)	a = 76.2, b = 137.1, c = 92.7, β = 103.8
Resolution range (Å)	50–2.8 (2.9–2.8)
Observed reflections	196103
Unique reflections	42775
Multiplicity	4.7 (4.0)
Completeness (%)	97.3 (94.2)
$R_{\rm merge}$† (%)	6.4 (31.6)
$\langle I/\sigma(I)\rangle$	18.3 (4.8)

† $R_{\rm merge} = \sum_{hkl}\sum_i |I_i(hkl) - \langle I(hkl)\rangle| / \sum_{hkl}\sum_i I_i(hkl)$, where $I_i(hkl)$ is the intensity of the ith observation of reflection hkl and $\langle I(hkl)\rangle$ is the average intensity of reflection hkl.

3. Results and discussion

The *Hs*-QPRTase crystals belonged to space group $P2_1$, with unit-cell parameters a = 76.2, b = 137.1, c = 92.7 Å, β = 103.8°. Assuming the presence of six molecules in the asymmetric unit, the calculated Matthews coefficient is 2.46 Å^3 Da^{-1}, which corresponds to a solvent content of 49.9% (Matthews, 1968). Molecular-replacement calculations were carried out with *MOLREP* (Vagin & Teplyakov, 2010) using the structure of the *Hs*-QPRTase–tartrate complex (PDB code 2jbm; Liu *et al.*, 2007) as a search model. The cross-rotation function for this model was calculated using data in the resolution range 15–4 Å and the first six peaks in the output appeared as distinct solutions. These six peaks grew more distinct in the translation calculations, with an overall correlation coefficient of 54.0% and an R factor of 48.2%. After refinement using the program *CNS* (Brünger *et al.*, 1998), the resultant electron-density map showed six molecules in an asymmetric unit and the quality of the initial map was high enough to build most of the residues. Model building and further refinement are ongoing.

This work was supported by grants from the Gwangju Institute of Science and Technology Systems Biology Infrastructure Establishment and the Korea Healthcare Technology R&D Project, Ministry for Health, Welfare and Family Affairs, Republic of Korea (A092006).

References

Brünger, A. T., Adams, P. D., Clore, G. M., DeLano, W. L., Gros, P., Grosse-Kunstleve, R. W., Jiang, J.-S., Kuszewski, J., Nilges, M., Pannu, N. S., Read,

R. J., Rice, L. M., Simonson, T. & Warren, G. L. (1998). *Acta Cryst.* D**54**, 905–921.
di Luccio, E. & Wilson, D. K. (2008). *Biochemistry*, **47**, 4039–4050.
Eads, J. C., Ozturk, D., Wexler, T. B., Grubmeyer, C. & Sacchettini, J. C. (1997). *Structure*, **5**, 47–58.
Feldblum, S., Rougier, A., Loiseau, H., Loiseau, P., Cohadon, F., Morselli, P. L. & Lloyd, K. G. (1988). *Epilepsia*, **29**, 523–529.
Foster, A. C. & Schwarcz, R. (1985). *J. Neurochem.* **45**, 199–205.
Foster, A. C., Whetsell, W. O., Bird, E. D. & Schwarcz, R. (1985). *Brain Res.* **336**, 207–214.
Foster, J. W. & Moat, A. G. (1980). *Microbiol. Rev.* **44**, 83–105.
Iwai, K. & Taguchi, H. (1974). *Biochem. Biophys. Res. Commun.* **56**, 884–891.
Kim, M. K., Im, Y. J., Lee, J. H. & Eom, S. H. (2006). *Proteins*, **63**, 252–255.
Liu, H., Woznica, K., Catton, G., Crawford, A., Botting, N. & Naismith, J. H. (2007). *J. Mol. Biol.* **373**, 755–763.
Matthews, B. W. (1968). *J. Mol. Biol.* **33**, 491–497.
Okuno, E. & Schwarcz, R. (1985). *Biochem. Biophys. Acta*, **841**, 112–119.
Okuno, E., White, R. J. & Schwarcz, R. (1988). *J. Biochem.* **103**, 1054–1059.
Otwinowski, Z. & Minor, W. (1997). *Methods Enzymol.* **276**, 307–326.
Schwarzenbacher, R. *et al.* (2004). *Proteins*, **55**, 768–771.
Sharma, V., Grubmeyer, C. & Sacchettini, J. C. (1998). *Structure*, **6**, 1587–1599.
Vagin, A. & Teplyakov, A. (2010). *Acta Cryst.* D**66**, 22–25.